Geophysical Research Letters

RESEARCH LETTER
10.1029/2023GL106856

Evaluation of Stratocumulus Evolution Under Contrasting Temperature Advections in CESM2 Through a Lagrangian Framework

Haipeng Zhang[1,2], **Youtong Zheng**[3,4], **and Zhanqing Li**[1,2]

[1]Department of Atmospheric and Oceanic Science, University of Maryland, College Park, MD, USA, [2]Earth System Science Interdisciplinary Center, University of Maryland, College Park, MD, USA, [3]Department of Earth and Atmospheric Science, University of Houston, Houston, TX, USA, [4]Institute of Climate and Atmospheric Science, University of Houston, Houston, TX, USA

Key Points:

- Community Earth System Model 2 simulates a too rapid decline in low-cloud fraction and cloud liquid water path when clouds experience cold-air advection
- It substantially overestimates increases in cloud liquid water path when clouds experience warm-air advection
- Utilizing an explainable machine learning methodology, the effects of meteorological factors on cloud evolution are assessed

Supporting Information:

Supporting Information may be found in the online version of this article.

Correspondence to:

Z. Li and Y. Zheng,
zhanqing@umd.edu;
yzheng18@uh.edu

Citation:

Zhang, H., Zheng, Y., & Li, Z. (2024). Evaluation of stratocumulus evolution under contrasting temperature advections in CESM2 through a Lagrangian framework. *Geophysical Research Letters*, *51*, e2023GL106856. https://doi.org/10.1029/2023GL106856

Received 17 OCT 2023
Accepted 30 JAN 2024

Abstract This study leveraged a Lagrangian framework to examine the evolution of stratocumulus clouds under cold and warm advections (CADV and WADV) in the Community Earth System Model 2 (CESM2) against observations. We found that CESM2 simulates a too rapid decline in low-cloud fraction (LCF) and cloud liquid water path (CLWP) under CADV conditions, while it better aligns closely with observed LCF under WADV conditions but overestimates the increase in CLWP. Employing an explainable machine learning approach, we found that too rapid decreases in LCF and CLWP under CADV conditions are related to overestimated drying effects induced by sea surface temperature, whereas the substantial increase in CLWP under WADV conditions is associated with the overestimated moistening effects due to free-tropospheric moisture and surface winds. Our findings suggest that overestimated drying effects of sea surface temperature on cloud properties might be one of crucial causes for the high equilibrium climate sensitivity in CESM2.

Plain Language Summary Stratocumulus clouds have extensive coverage over the oceans and modulate the climate system by efficiently reflecting incoming solar radiation back to space. However, their simulations in climate models are challenging due to complex meteorological controls, in which temperature advection is one of the most uncertain controlling factors. To enhance our understanding, we examine the stratocumulus evolution influenced by cold-advection (CADV) and warm-advection (WADV) in the midlatitudes in a climate model, CESM2. A too rapid decrease in low-cloud fraction (LCF) and cloud liquid water path (CLWP) is erroneously simulated under CADV conditions, while an increase in CLWP is substantially overestimated under WADV conditions. Using an explainable machine learning approach, these errors are found to be caused by the amplified drying or moistening effects due to improper treatments of meteorological controls on clouds in CESM2. This study suggests that these misrepresentations of cloud physics in the midlatitudes should be imperatively improved to reduce climate prediction uncertainties.

1. Introduction

Marine stratocumulus (Sc) clouds have the most extensive coverage over the Earth's surface compared to other cloud types (Hahn & Warren, 2007; Wood, 2012), significantly influencing the climate system. They play a crucial role in climate prediction uncertainties (Cess et al., 1990; Soden & Vecchi, 2011; Vial et al., 2013; H. Zhang et al., 2018; M. Zhang et al., 2013).

Sc clouds are controlled by large-scale meteorological factors (MFs), such as inversion strength (measured by the estimated inversion strength or EIS; Wood & Bretherton, 2006), sea surface temperature (SST), low-level temperature advection (T_{adv}), large-scale vertical velocity (ω), free-tropospheric (FT) moisture, and surface wind speed (U). Among those, T_{adv} is the least understood one (Seethala et al., 2015). For example, Myers and Norris (2015) revealed that the sensitivity of shortwave (SW) cloud radiative effect (CRE) to T_{adv} exhibits the greatest uncertainty among 11 CMIP3 and 14 CMIP5 models, while the sensitivity of SW CRE to SST, EIS, FT moisture, and subsidence compare well with observations. To enhance our understanding of T_{adv}'s influence, it is crucial to investigate the evolution of cloud properties and marine-boundary-layer (MBL) structures as Sc clouds advect under different T_{adv} conditions. A well-known situation is the stratocumulus-to-cumulus (Sc-to-Cu) transition, that is, the MBL evolves from a well-mixed layer topped with extensive Sc capped by a strong inversion into a deeper and decoupled layer dominated by cumulus clouds (Cu) under a weak inversion (B.

Albrecht et al., 2019; B. A. Albrecht et al., 1995; Bretherton et al., 1999; Wyant et al., 1997). This transition mostly takes place over the subtropics, driven by trade winds that move Sc clouds toward warmer water (i.e., experiencing cold-air advection or CADV). While numerous studies have focused on Sc evolution under CADV conditions, the dynamics of Sc clouds experiencing warm-air advection (warm air moving over colder SSTs; WADV), prevalent in midlatitudes, have received less attention. Observations from two mid-latitude field campaigns revealed that over 25% of single-layer Sc clouds experienced WADV (Zheng et al., 2020). Additionally, findings from climate models and satellite observations indicated that the occurrence probability of Sc clouds experiencing WADV is around 30%, close to those experiencing CADV in the midlatitudes (Figure S3 in Supporting Information S1). Given the potential climatological significance of Sc clouds under WADV conditions, it is crucial to further our understanding of this cloud regime and its representations in global climate models (GCMs).

Sc clouds demonstrate distinct dynamics in their coupling with the surface under varying T_{adv} conditions. In CADV, the stably stratified MBL is characterized by cumulus coupling (Bretherton & Wyant, 1997). However, in WADV, the stratocumulus deck shows a complete decoupling from the sea surface, indicated by weakly negative buoyancy flux throughout the subcloud layer (Zheng et al., 2021). Compared to CADV, the decoupling in WADV, that is, suppressed surface fluxes, tends to prolong the persistence of Sc decks, as observed by Zheng and Li (2019). The mechanism was revealed by H. Zhang et al. (2023) using large-eddy simulations (LESs), finding that reduced entrainment drying due to decoupling helps sustain cloud decks in WADV. Due to different decoupling features, Sc cloud responses to environmental factors also exhibit distinct behaviors between CADV and WADV conditions. H. Zhang et al. (2023) found that cloud lifetime is more sensitive to variations in FT moisture under WADV conditions compared to its cold counterpart as WADV-induced complete decoupling minimizes the surface forcing effects, yielding the dominant influence of FT moisture. These findings highlight the markedly distinct impacts of physical processes on cloud properties under two contrasting T_{adv} conditions. Accurate representation of those physical controls under CADV and WADV scenarios is crucial to mitigating cloud feedback uncertainties pertaining to T_{adv}. It is, therefore, necessary to examine how well the physical processes governing Sc evolution under these contrasting T_{adv} conditions are represented in climate models.

In that regard, a novel Lagrangian framework is employed to compare models and observations (Christensen et al., 2022; Eastman et al., 2021). This approach samples parcels as they evolve in time and space, allowing the exploration of the causal relationships between clouds and their controlling factors on daily timescales. To examine the meteorological controls on clouds, an explainable machine learning approach called SHapley Additive exPlanations (SHAP; Lundberg & Lee, 2017; Lundberg et al., 2018) is utilized to quantify the individual contribution of each influencing factor to cloud property changes. We shall examine cloud evolutions under two contrasting T_{adv} conditions and their meteorological controls in the Community Earth System Model 2 against observational data through a Lagrangian framework.

2. Methodology

2.1. Climate Model

The Community Earth System Model Version 2.2.0 (CESM2; Danabasoglu et al., 2020) is used. Its atmospheric component, the Community Atmosphere Model Version 6 (CAM6; Bogenschutz et al., 2017), implements a higher-order turbulence closure scheme named the Cloud Layers Unified By Bi-normals (CLUBB; Golaz et al., 2002a, 2002b; Larson & Golaz, 2005; Larson et al., 2002, 2012) that replaces the separate treatments of boundary layer turbulence, large-scale cloud macrophysics, and shallow convection employed in the previous version (CAM5). This new unified scheme has been shown to significantly improve the simulations of low clouds, especially over the Sc-to-Cu transition regime in CAM5 (Bogenschutz et al., 2013). CAM6 also adopts the Zhang-McFarlane scheme (G. J. Zhang & McFarlane, 1995) for deep convective processes, the RRTMG scheme for radiation (Iacono et al., 2008), and the improved Morrison–Gettelman scheme for microphysics (Gettelman & Morrison, 2015). A horizontal resolution of $0.9° \times 1.25°$ is used with 32 vertical layers. The model is initiated on 1 January 2010 through the CESM2 AMIP6 restart files and is run for 2 years. Instantaneous data are outputted every 6 hr for analysis. Monthly varying SSTs are prescribed by HadISST (Rayner et al., 2003). A satellite simulator, the Cloud Feedback Model Intercomparison Project (CFMIP) Observation Simulator Package (COSP; Bodas-Salcedo et al., 2011) is enabled for the CESM2 cloud fraction. The modeled low-cloud fraction (LCF) is determined as the maximum cloud fraction below 700 hPa.

2.2. Satellite and Reanalysis Data

The CERES SYN Ed4 product provides observational (1° latitude by 1° longitude resolved hourly) LCF and cloud liquid water path (CLWP) over the period of 2010–2011. This product utilizes 16 geostationary satellites. To ensure consistency across the various satellite sensors, the instrument channels are cross-calibrated to match the cloud retrievals from the MODIS collection 5 product (Doelling et al., 2013).

The fifth-generation ECMWF reanalysis data (ERA5; Hersbach et al., 2020) provide meteorological variables such as horizontal wind fields. The 6-hourly data are used, with the grid resolution of 0.9° × 1.25°, as for the CESM2 outputs.

2.3. Lagrangian Framework

We examine cloud evolution over 36 hr along Lagrangian trajectories, driven by the isobaric winds at 925 hPa from CESM2 and ERA5 (used for tracking observations), assuming that this level approximates the cloud level within the MBL (Eastman & Wood, 2018). This study is focused on the mid-latitude oceans (30–60°S/N), where WADV and CADV are both prevalent. In these regions, the starting point of trajectories are sampled at an equal distance of 200 km, yielding 8032 points in total (see Figure S1 in Supporting Information S1). For each starting point, the 36-hr forward trajectories are computed every 6 hr for the years 2010–2011 (an example is illustrated in Figure S2 in Supporting Information S1). Cloud properties (LCF and CLWP) and meteorological variables are tracked along Lagrangian trajectories for analysis in CESM2 and observations, respectively.

WADV events typically occur in the warm sections of tropical cyclones, where large-scale updrafts favor the formation of middle and high clouds, obscuring the observations of low clouds (Wall et al., 2017). To minimize the impact of mid- and high-level cloud contamination, we selected those trajectories that begin with single-layer Sc clouds with cloudiness greater than 0.5 (following Zheng et al. (2020)) and mid- and high-level cloudiness less than 0.05. Moreover, we choose the trajectories occurring under CADV and WADV conditions, through the criterion that the linearized temporal rate of SSTs along the trajectory is non-zero at a significance level of 0.05. As a result, for CESM2, ∼0.4 million trajectories are selected under CADV conditions and ∼0.1 million under WADV conditions. For observations, ∼0.7 and ∼0.1 million trajectories are selected for CADV and WADV, respectively.

2.4. Machine Learning Model and Its Interpretability Analysis

Cloud evolution is primarily governed by large-scale MFs. To examine the meteorological controls, an interpretable machine learning model called the eXtreme Gradient Boosting Decision Tree (XGBoost; T. Chen & Guestrin, 2016) is used to predict LCF or CLWP variations along trajectories with chosen large-scale MFs. The interpretation of XGBoost prediction results by SHAP analysis reveals the individual effect of each factor on cloud variations, which is the primary focus of model-observation comparison in this study.

We use the 36-hr variations in LCF or CLWP as the predictands (using 24-hr variations does not change our main findings). The chosen large-scale MFs are recommended by previous studies (Bretherton, 2015; Qu et al., 2015; Sandu et al., 2010): EIS, SST, FT moisture at 700 hPa (q_{700}), moisture difference between 700 hPa and 1,000 hPa (dq), large-scale subsidence rate at 700 hPa (ω_{700}), and surface wind speed at 925 hPa (U_{925}). The initial values and 36-hr variations in these MFs are denoted as MF_0 and ΔMF respectively. We employed both as predictors. Physically speaking, the MF_0 and ΔMF represent cloud controllers at different time scales: the MF_0 represents synoptic scale influence (i.e., cloud responds to the upstream meteorological through a multi-day memory or long-term impact of an MF) and the ΔMF represents a more immediate effect (short-term impact of an MF).

In addition to MFs, initial values in cloud properties are also used as predictors, because of "regression to the mean" (also called "regression artifact"), that is, trajectories starting with higher LCF (CLWP) values tend to show a more noticeable decrease in LCF (CLWP) over time (Eastman et al., 2021). The effects of regression artifacts can be easily isolated from physical controls on cloud variations via SHAP analysis. XGBoost models are trained separately for CESM2 modeling results and observations under two T_{adv} conditions. Training details can be found in Text S1 in Supporting Information S1. The machine learning model merits here because it accounts for the non-linear effects between MFs, exhibiting higher explained variance score compared to multiple linear regression (MLR) models (compare Table S1 in Supporting Information S1 with Table S2 in Supporting Information S1).

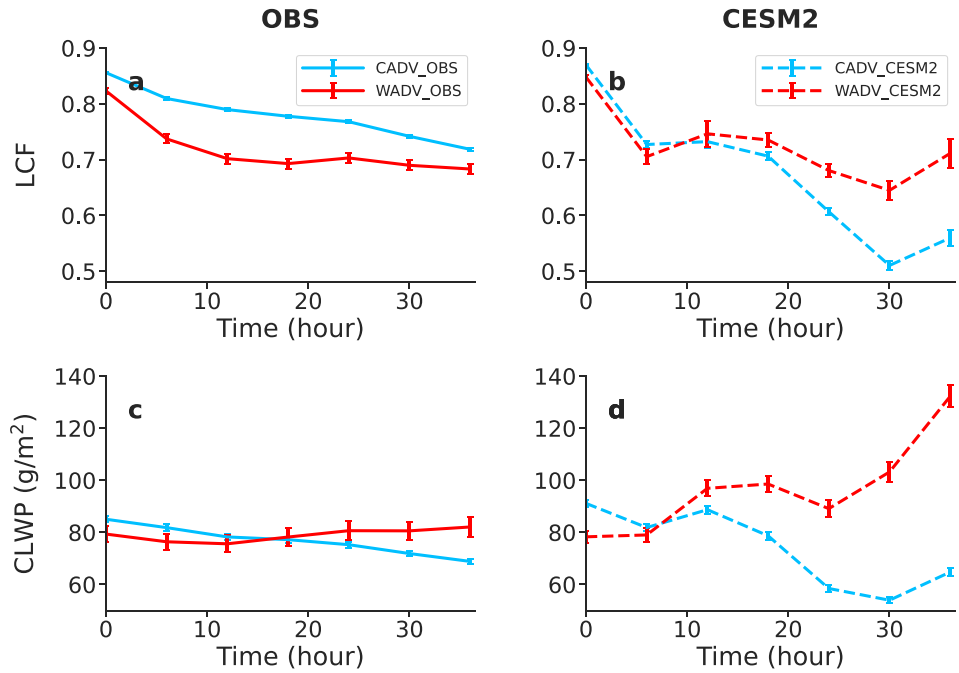

Figure 1. Time series of the ensemble-mean (a) low-cloud fraction (LCF) and (c) cloud liquid water path (CLWP) under CADV (blue) and WADV (red) conditions for all selected trajectory cases in observations. Panels (b, d) show the same ones, but for CESM2. The error bars represent the expanded standard error (SE) of 10 for visualization. The standard error is calculated as SE = $\sigma/\sqrt{n}$ with σ the standard deviation and n the total sample size.

To determine the individual effect of each MF on cloud variations, we employ a statistical approach from cooperative game theory, SHAP (SHapley Additive exPlanations; Lundberg & Lee, 2017; Lundberg et al., 2018) to interpret the machine learning model behavior. SHAP analysis explains a model's individual output (e.g., LCF variations) as a sum of the contributions of each predictor (e.g., MFs) and the mean predicted value through an explanation model, which can be expressed as:

$$y = \bar{y} + \sum_i \phi_i, \tag{1}$$

where y is the final prediction for one case, $\bar{y}$ is the average prediction across all cases, and ϕ_i is the marginal contribution of the ith feature to the prediction for this case (called SHAP values). To calculate SHAP values, an efficient and exact algorithm, TreeSHAP, is adopted, which was developed for tree ensemble models using the conditional expectation to estimate the effects of predictors (Lundberg et al., 2018, 2020). In this study, MFs with larger absolute SHAP values have a greater contribution to predicted LCF/CLWP variations. The sensitivity of an MF's SHAP values to this factor reveals its individual meteorological control on cloud evolution. Figures S4–S7 in Supporting Information S1 show the SHAP values as functions of initial values and 36-hr changes in MFs. The predictant variables, LCF/CLWP variations, are linearly transformed to between 0 and 1. The unit of SHAP values is thus 1.0.

3. Results

3.1. Evolution of Cloud Properties

Figure 1 compares the ensemble-mean evolution of LCF and CLWP along the selected trajectories between observational and CESM2 modeling results under two T_{adv} conditions. For cloud decks experiencing CADV, observations show a persistent reduction in both LCF and CLWP (Figures 1a and 1c). CESM2 also shows similar trends (Figures 1b and 1d) but with some oscillations over time. However, the modeled decrease in cloud fraction and cloud water (by around 0.35 and 30 g/m^2 respectively) exhibits a significantly steeper decline compared to observations (by 0.13 and 13 g/m^2), indicating that the issue of too rapid Sc-to-Cu transitions in CESM models persists, despite the improvements made by the implementation of CLUBB (Bogenschutz et al., 2013). For

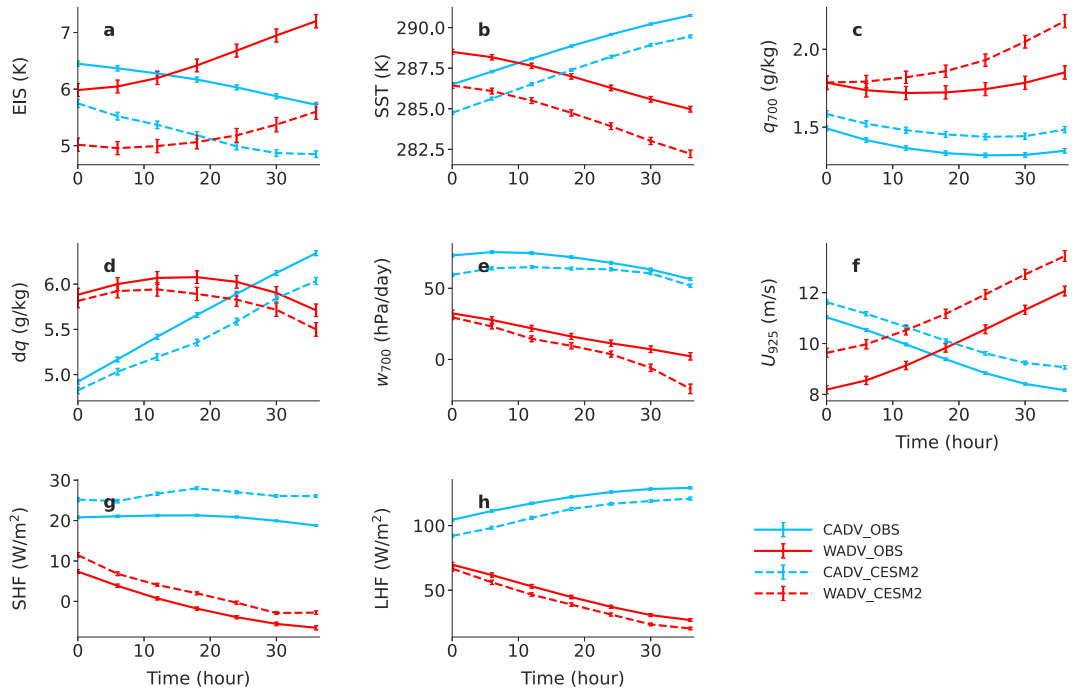

Figure 2. Time series of the ensemble-mean (a) EIS, (b) SST, (c) q_{700}, (d) dq, (e) w_{700}, (f) U_{925}, (g) sensible heat flux, and (h) latent heat flux under CADV (blue) and WADV (red) conditions for all selected trajectory cases in observations (solid lines) and CESM2 (dashed lines), respectively. The error bars represent the expanded standard error of 10 for visualization.

WADV, observations show decreasing LCF and increasing CLWP trends. Similar trends are observed in CESM2 but with different amplitudes of variations. The modeled decrease in LCF is generally consistent with that in observations (by around 0.15), whereas the increase in CLWP is significantly overestimated by CESM2 (by 50 g/m^2) as opposed to the flat increase in observations.

Two questions arise here: What causes the too rapid Sc-to-Cu transition under CADV conditions in CESM2? Why does CESM2 simulate a greater increase in CLWP under WADV conditions than observations? We address these questions by examining modeled individual effects of MFs on the evolution of cloud properties through an explainable machine learning approach.

3.2. Evolution of Meteorological Factors

Figure 2 shows the time series of MFs. Generally, observations and CESM2 display similar trends for these variables. We first examine the trend of these MFs under CADV conditions, marked by blue lines in Figure 2. Mean EIS tends to decrease over time (Figure 2a), as a result of increased SST (Figure 2b) or enhanced surface fluxes (dominated by latent heat fluxes in Figures 2g and 2h). For background FT moisture changes, we find a large drop and a subsequent slight increase in q_{700} (Figure 2c). dq tends to increase sharply (Figure 2d), indicating that entrainment is drying clouds more efficiently (see the entrainment drying term in Equation 1 in H. Zhang et al. (2023)). Meanwhile, drying effects by subsidence tend to become weaker as ω_{700} is decreasing (Figure 2e), resulting in less drying air being brought downward. Surface winds show a decreasing trend (Figure 2f), and thus the wind-shear-driven turbulence near the surface might weaken.

Compared to CADV, some key MFs exhibit the opposite trends under WADV conditions (red lines in Figure 2), which are essentially caused by the reversed SST forcings (Figure 2b). Specifically, with decreasing SST, the surface-atmosphere interface becomes more stabilized, which increasingly suppresses surface fluxes (Figures 2g and 2h). dq and surface winds show the opposite trends compared to those under CADV conditions as well. Similar trends are only found for q_{700} and ω_{700}. But it is noteworthy that under WADV conditions CESM2 simulates a much more rapid increase in q_{700} compared to observations (Figure 2c), possibly related to the more rapid drop in the simulated ω_{700} (Figure 2e). This misrepresented increase in q_{700} partly explains the too rapid increase in CLWP under WADV conditions.

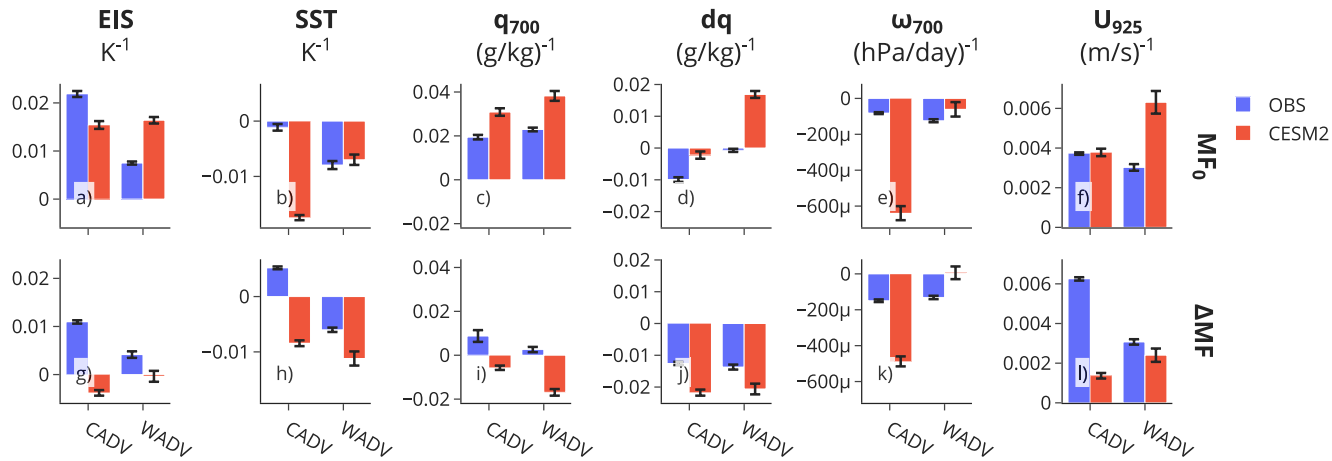

Figure 3. Barplot of the sensitivity of SHAP values to initial values (MF_0; the first row) and 36-hr variations in meteorological factors (ΔMF; the second row) when predicting LCF variations, derived from observational data (blue) and CESM2 simulation results (red) under CADV/WADV conditions. This sensitivity is determined by initially sorting a predictor's SHAP values into 15 equal bins based on the values of this predictor, followed by conducting a least squares regression on these binned averages against the predictor. The slope of the regression line quantifies the sensitivity (see its unit below the MF name), and its standard error is represented by the error bar. μ means 1×10^{-6}.

3.3. Meteorological Controls on Cloud Evolution

Figure 3 summarizes the individual effects of each MF on LCF variations. The effects of an MF are classified into the long-term (background) effect and the rapid effect, quantified by the slopes of the changes of SHAP values with MF_0 and ΔMF, respectively. Before we address the two questions raised in Section 3.1, we first summarize the observed controls of different predictors on cloud evolutions. Overall, observations show results consistent with our previous understandings. For instance, a larger EIS tends to increase LCF because stronger cloud-top inversion caps more moisture in the MBL (Bretherton et al., 2013). Increased SST dries clouds because the corresponding increased LHF enhances the buoyancy-driven mixing of dry air in the free troposphere into the boundary layer or entrainment drying (Rieck et al., 2012). But a reversed influence is observed for its rapid effect under CADV conditions (see the left blue bar in Figure 3h), which warrants further investigation. The influence of free-troposphere moisture (q_{700}) is still controversial. Some studies found that more emissive free-troposphere desiccates clouds owing to weaker moisture transport by turbulent/convective mixing (Bretherton, 2015; Christensen et al., 2013) while others revealed that it increases clouds due to less entrainment drying by offsetting cloud-top radiative cooling (Myers & Norris, 2016; van der Dussen et al., 2015). Our findings corroborate the second mechanism. An increase in *dq* is expected to decrease clouds as it makes entrainment drying more efficient. Stronger subsidence tends to dry clouds as it brings more dry air from the free troposphere downward (van der Dussen et al., 2016). Enhanced winds tend to moisten clouds as enhanced surface driven shear mixing increases latent heat flux and clouds (Bretherton et al., 2013; Brueck et al., 2015). The relative contributions of these factors are shown in Figure S8 in Supporting Information S1. Our findings suggest that EIS is the most crucial meteorological determinant for LCF evolution under CADV conditions with a particularly pronounced long-term impact, whereas SST stands out as the most influential factor under WADV conditions.

To answer the first question, we dive into the investigation of modeling errors that lead to a rapid decrease in LCF under CADV conditions (Figure 1b). One robust cause of the LCF rapid decrease is due to an overestimation of SST-induced drying effects. This overestimation is notably observed for the long-term or background impact of SST (Figure 3b). That makes CESM2 tend to simulate a larger decrease in LCF over time given the close initial conditions between simulations and observations. Moreover, the short-term drying effect induced by SST is also overestimated (Figure 3h), further accentuating the LCF decline given the rising SST trend (Figure 2b). However, some MFs display competing effects between long-term and short-term impacts, complicating the analysis. For instance, the long-term moistening impact of EIS is underestimated, thereby amplifying a rapid decrease in simulated LCF, but its underestimated short-term moistening impact slows down the LCF decrease as EIS decreases over time (see blue lines in Figure 2a). Similar offsetting dynamics are observed for other MFs. Factors like the overestimated short-term drying effect of *dq* and the overestimated long-term drying impact of subsidence contribute to the rapid decrease in simulated LCF. However, these impacts are often counterbalanced by opposing

10.1029/2023GL106856

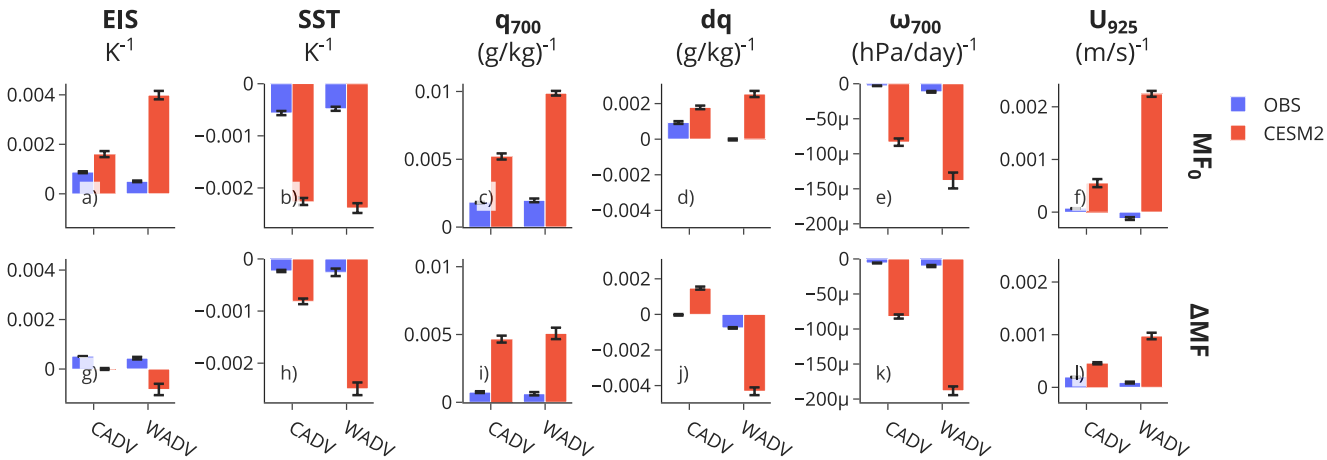

Figure 4. Same as Figure 3, but for CLWP variations.

forces within the same MF, making net effect assessments intricate. In contrast, under WADV conditions, many of the errors simulated under CADV conditions are substantially diminished, such as the short-term effects of EIS, SST, ω_{700} and U_{925}. These make substantial improvements in LCF simulations under WADV conditions.

The observed meteorological controls on LWP evolution (Figure 4) are similar to those discussed for LCF. To answer the second question, we probe into the causes of the substantial increase in CLWP under WADV conditions (Figure 1d). Compared to CADV, modeling errors of meteorological effects are larger under WADV conditions, particularly with factors like EIS, SST, q_{700}, w_{700}, and U_{925}. Examining these errors, we find that the overestimated moistening effects of q_{700} (Figures 4c and 4i) and U_{925} (Figures 4f and 4l) robustly explain the significant increase in simulated CLWP since no competing effects are observed. Additionally, the overestimated long-term moistening effects induced by EIS and the overestimated short-term drying effects induced by SST, dq, and w_{700} contribute to CLWP increase, although these are somewhat moderated by corresponding counter-effects within each MF.

4. Implications for High ECS in CESM2

Gettelman et al. (2019) and Bacmeister et al. (2020) have shown that the higher equilibrium climate sensitivity (ECS) of 5.3 K in CESM2 compared to CESM1 mainly results from increased cloud feedback. A key contributor to increased cloud feedback is the cloud-phase feedback (Tan et al., 2016). CESM2's correction of supercooled liquid underestimation in CESM1 leads to a weaker negative cloud-phase feedback, hence contributing to the higher ECS (Bjordal et al., 2020; Gettelman et al., 2019). In addition to mixed-phase ice nucleation, misrepresentations of other physical processes could also contribute to the increased ECS. Our findings, exemplified in Figures 3 and 4, show an overall overestimated drying effect induced by SST in midlatitudes across varied timescales and T_{adv} conditions, contributing to an increase in positive cloud feedback. For instance, the overestimation biases shown in Figure 3b for CADV suggest that in a warmer climate, a rise in background SST tends to amplify the reduction in LCF along the Sc-to-Cu transition, thereby exacerbating global warming. One potential reason for the overestimated drying effects is that in CESM2 an increase in SST causes an excessive enhancement of buoyancy-driven mixing of dry free tropospheric air into the MBL. This suggests that some CLUBB parameters influencing the boundary layer mixing like C7/C7b (Guo et al., 2015) should be tuned to decrease the sensitivity of LCF (or CLWP) to SST variations. Furthermore, the model overrepresents long-term moistening effects from FT moisture and surface winds on cloud properties under CADV and WADV conditions. The overestimated moistening biases caused by surface winds in the model may stem from CLUBB's overly efficient turbulence production due to near-surface wind shears, suggesting that pressure changes due to wind shear (see Equation 4.11 in Larson (2022)) might be too large, hence producing excessive clouds. Given the declining trend in FT moisture and surface winds in a warming climate in midlatitudes in GCMs (Myers et al., 2021), these simulated stronger meteorological effects also hint at greater positive feedbacks, which shed light on the increased ECS in CESM2.

5. Summary

This study evaluates the evolution of marine stratocumulus clouds and associated meteorological controls under two contrasting temperature advections—cold-air advection (CADV) and warm-air advection (WADV)—in CESM2 against observations through a Lagrangian framework. Our investigation reveals that under CADV conditions, CESM2 simulates a too rapid stratocumulus-to-cumulus transition regarding low-cloud fraction (LCF) and cloud liquid water path (CLWP). In contrast, a closer alignment of LCF evolution with observations is exhibited under WADV conditions, but with a significant overestimation of CLWP increases. Employing an explainable machine learning approach, we probe into the potential causes of misrepresented cloud evolution by examining the effects of meteorological factors. The simulated rapid reduction in LCF and CLWP under CADV conditions is found to be related to the overestimated drying effects induced by sea surface temperature (SST), whereas the substantial increase in CLWP is associated with the overestimated moistening effects of free-tropospheric moisture and surface winds. Other meteorological factors may also contribute to the bias, but with uncertainties due to the competing effect between long-term and short-term impact within each factor. Moreover, our findings suggest that overestimated drying effects due to SST and moistening effects from free-tropospheric moisture and surface winds might contribute to the high equilibrium climate sensitivity in CESM2. This study showcases a useful machine-learning-based framework for assessing the representation of cloud physics in climate models, offering the potential for its application in CMIP6 model comparisons regarding meteorological controls on clouds in future studies.

Data Availability Statement

The CESM2 model code is available at Danabasoglu et al. (2020). The ERA5 reanalysis data are available at Hersbach et al. (2020). The CERES SYN Ed4 products are available at CERES Science Team (2021). CESM2 simulation results are available upon request via email.

Acknowledgments

This study is supported by the Department of Energy (DOE) Atmospheric System Research program (DESC0022919) and the National Science Foundation (AGS2126098). YZ is supported by the DOE Early Career grant (DE-SC0024185). We acknowledge high-performance computing support from Cheyenne (https://doi.org/10.5065/D6RX99HX) provided by NCAR's Computational and Information Systems Laboratory, sponsored by the National Science Foundation. We thank Ryan Eastman for providing MATLAB codes for trajectory calculations. We thank two anonymous reviewers for their constructive comments, which considerably improved the quality of the manuscript.

References

Albrecht, B., Ghate, V., Mohrmann, J., Wood, R., Zuidema, P., Bretherton, C., et al. (2019). Cloud System Evolution in the Trades (CSET): Following the evolution of boundary layer cloud systems with the NSF–NCAR GV. *Bulletin of the American Meteorological Society*, *100*(1), 93–121. https://doi.org/10.1175/BAMS-D-17-0180.1

Albrecht, B. A., Bretherton, C. S., Johnson, D., Scubert, W. H., & Frisch, A. S. (1995). The Atlantic stratocumulus transition experiment—ASTEX. *Bulletin of the American Meteorological Society*, *76*(6), 889–904. https://doi.org/10.1175/1520-0477(1995)076<0889:TASTE>2.0.CO;2

Bacmeister, J. T., Hannay, C., Medeiros, B., Gettelman, A., Neale, R., Fredriksen, H. B., et al. (2020). CO_2 increase experiments using the CESM: Relationship to climate sensitivity and comparison of CESM1 to CESM2. *Journal of Advances in Modeling Earth Systems*, *12*(11), 1–39. https://doi.org/10.1029/2020MS002120

Bjordal, J., Storelvmo, T., Alterskjær, K., & Carlsen, T. (2020). Equilibrium climate sensitivity above 5°C plausible due to state-dependent cloud feedback. *Nature Geoscience*, *13*(11), 718–721. https://doi.org/10.1038/s41561-020-00649-1

Bodas-Salcedo, A., Webb, M. J., Bony, S., Chepfer, H., Dufresne, J.-L., Klein, S. A., et al. (2011). COSP: Satellite simulation software for model assessment. *Bulletin of the American Meteorological Society*, *92*(8), 1023–1043. https://doi.org/10.1175/2011BAMS2856.1

Bogenschutz, P. A., Gettelman, A., Hannay, C., Larson, V. E., Neale, R. B., Craig, C., & Chen, C.-C. (2017). The path to CAM6: Coupled simulations with CAM5.4 and CAM5.5. *Geoscientific Model Development Discussions*, 1–38. https://doi.org/10.5194/gmd-2017-129

Bogenschutz, P. A., Gettelman, A., Morrison, H., Larson, V. E., Craig, C., & Schanen, D. P. (2013). Higher-order turbulence closure and its impact on climate simulations in the community atmosphere model. *Journal of Climate*, *26*(23), 9655–9676. https://doi.org/10.1175/JCLI-D-13-00075.1

Bretherton, C. S. (2015). Insights into low-latitude cloud feedbacks from high-resolution models. *Philosophical Transactions of the Royal Society A: Mathematical, Physical & Engineering Sciences*, *373*(2054), 20140415. https://doi.org/10.1098/rsta.2014.0415

Bretherton, C. S., Blossey, P. N., & Jones, C. R. (2013). Mechanisms of marine low cloud sensitivity to idealized climate perturbations: A single-LES exploration extending the CGILS cases. *Journal of Advances in Modeling Earth Systems*, *5*(2), 316–337. https://doi.org/10.1002/jame.20019

Bretherton, C. S., Krueger, S. K., Wyant, M. C., Bechtold, P., Van Meijgaard, E., Stevens, B., & Teixeira, J. (1999). A GCSS boundary-layer cloud model intercomparison study of the first ASTEX Lagrangian experiment. *Boundary-Layer Meteorology*, *93*(3), 341–380. https://doi.org/10.1023/A:1002005429969

Bretherton, C. S., & Wyant, M. C. (1997). Moisture transport, lower-tropospheric stability, and decoupling of cloud-topped boundary layers. *Journal of the Atmospheric Sciences*, *54*(1), 148–167. https://doi.org/10.1175/1520-0469(1997)054<0148:MTLTSA>2.0.CO;2

Brueck, M., Nuijens, L., & Stevens, B. (2015). On the seasonal and synoptic time-scale variability of the North Atlantic trade wind region and its low-level clouds. *Journal of the Atmospheric Sciences*, *72*(4), 1428–1446. https://doi.org/10.1175/JAS-D-14-0054.1

CERES Science Team. (2021). The CERES SYN1deg Ed4A products [Dataset]. NASA Atmospheric Science Data Center (ASDC). Retrieved from https://ceres-tool.larc.nasa.gov/ord-tool/jsp/SYN1degEd41Selection.jsp

Cess, R. D., Potter, G. L., Blanchet, J. P., Boer, G. J., Del Genio, A. D., Deque, M., et al. (1990). Intercomparison and interpretation of climate feedback processes in 19 atmospheric general circulation models. *Journal of Geophysical Research*, *95*(D10), 16601–16615. https://doi.org/10.1029/jd095id10p16601

Chen, T., & Guestrin, C. (2016). XGBoost: A scalable tree boosting system. In *Proceedings of the 22nd ACM SIGKDD international conference on knowledge discovery and data mining* (Vol. 42, pp. 785–794). ACM. https://doi.org/10.1145/2939672.2939785

Christensen, M. W., Carrió, G. G., Stephens, G. L., & Cotton, W. R. (2013). Radiative impacts of free-tropospheric clouds on the properties of marine stratocumulus. *Journal of the Atmospheric Sciences*, *70*(10), 3102–3118. https://doi.org/10.1175/JAS-D-12-0287.1

Christensen, M. W., Ma, P., Wu, P., Varble, A. C., Mülmenstädt, J., & Fast, J. D. (2022). Evaluation of aerosol-cloud interactions in E3SM using a Lagrangian framework (pp. 1–38).

Danabasoglu, G., Lamarque, J.-F., Bacmeister, J., Bailey, D. A., DuVivier, A. K., Edwards, J., et al. (2020). The Community Earth System Model Version 2 (CESM2) [Software]. UCAR, *12*. https://doi.org/10.1029/2019ms001916

Doelling, D. R., Loeb, N. G., Keyes, D. F., Nordeen, M. L., Morstad, D., Nguyen, C., et al. (2013). Geostationary enhanced temporal interpolation for ceres flux products. *Journal of Atmospheric and Oceanic Technology*, *30*(6), 1072–1090. https://doi.org/10.1175/JTECH-D-12-00136.1

Eastman, R., Terai, C. R., Grosvenor, D. P., & Wood, R. (2021). Evaluating the Lagrangian evolution of subtropical low clouds in GCMs using observations: Mean evolution, time scales, and responses to predictors. *Journal of the Atmospheric Sciences*, *78*(2), 553–572. https://doi.org/10.1175/JAS-D-20-0178.1

Eastman, R., & Wood, R. (2018). The competing effects of stability and humidity on subtropical stratocumulus entrainment and cloud evolution from a Lagrangian perspective. *Journal of the Atmospheric Sciences*, *75*(8), 2563–2578. https://doi.org/10.1175/JAS-D-18-0030.1

Gettelman, A., Hannay, C., Bacmeister, J. T., Neale, R. B., Pendergrass, A. G., Danabasoglu, G., et al. (2019). High climate sensitivity in the Community Earth System Model Version 2 (CESM2). *Geophysical Research Letters*, *46*(14), 8329–8337. https://doi.org/10.1029/2019GL083978

Gettelman, A., & Morrison, H. (2015). Advanced two-moment bulk microphysics for global models. Part I: Off-line tests and comparison with other schemes. *Journal of Climate*, *28*(3), 1268–1287. https://doi.org/10.1175/JCLI-D-14-00102.1

Golaz, J.-C., Larson, V. E., & Cotton, W. R. (2002a). A PDF-based model for boundary layer clouds. Part I: Method and model description. *Journal of the Atmospheric Sciences*, *59*(24), 3540–3551. https://doi.org/10.1175/1520-0469(2002)059<3540:APBMFB>2.0.CO;2

Golaz, J.-C., Larson, V. E., & Cotton, W. R. (2002b). A PDF-based model for boundary layer clouds. Part II: Model results. *Journal of the Atmospheric Sciences*, *59*(24), 3552–3571. https://doi.org/10.1175/1520-0469(2002)059<3552:APBMFB>2.0.CO;2

Guo, Z., Wang, M., Qian, Y., Larson, V. E., Ghan, S. J., Ovchinnikov, M., et al. (2015). Parametric behaviors of CLUBB in simulations of low clouds in the Community Atmosphere Model (CAM). *Journal of Advances in Modeling Earth Systems*, *7*(3), 1005–1025. https://doi.org/10.1002/2014MS000405

Hahn, C. J., & Warren, S. G. (2007). *A gridded climatology of clouds over land (1971–1996) and ocean (1954–1997) from surface observations worldwide* (Vol. 55). Oak Ridge National Laboratory, Carbon Dioxide Information Analysis Center. https://doi.org/10.3334/CDIAC/cli.ndp026e

Hersbach, H., Bell, B., Berrisford, P., Zhang, M., Horányi, A., Muñoz-Sabater, J., et al. (2020). The ERA5 global reanalysis [Dataset]. Copernicus Climate Change Service (C3S) Climate Data Store (CDS). https://doi.org/10.24381/cds.bd0915c6

Iacono, M. J., Delamere, J. S., Mlawer, E. J., Shephard, M. W., Clough, S. A., & Collins, W. D. (2008). Radiative forcing by long-lived greenhouse gases: Calculations with the AER radiative transfer models. *Journal of Geophysical Research*, *113*(13), 2–9. https://doi.org/10.1029/2008JD009944

Larson, V. E. (2022). CLUBB-SILHS: A parameterization of subgrid variability in the atmosphere. https://doi.org/10.48550/arXiv.1711.03675

Larson, V. E., & Golaz, J.-C. (2005). Using probability density functions to derive consistent closure relationships among higher-order moments. *Monthly Weather Review*, *133*(4), 1023–1042. https://doi.org/10.1175/MWR2902.1

Larson, V. E., Golaz, J.-C., & Cotton, W. R. (2002). Small-scale and mesoscale variability in cloudy boundary layers: Joint probability density functions. *Journal of the Atmospheric Sciences*, *59*(24), 3519–3539. https://doi.org/10.1175/1520-0469(2002)059<3519:SSAMVI>2.0.CO;2

Larson, V. E., Schanen, D. P., Wang, M., Ovchinnikov, M., & Ghan, S. (2012). PDF parameterization of boundary layer clouds in models with horizontal grid spacings from 2 to 16 km. *Monthly Weather Review*, *140*(1), 285–306. https://doi.org/10.1175/MWR-D-10-05059.1

Lundberg, S. M., Erion, G., Chen, H., DeGrave, A., Prutkin, J. M., Nair, B., et al. (2020). From local explanations to global understanding with explainable AI for trees. *Nature Machine Intelligence*, *2*(1), 56–67. https://doi.org/10.1038/s42256-019-0138-9

Lundberg, S. M., Erion, G. G., & Lee, S.-I. (2018). Consistent individualized feature attribution for tree ensembles. Retrieved from http://arxiv.org/abs/1802.03888

Lundberg, S. M., & Lee, S. I. (2017). A unified approach to interpreting model predictions. *Advances in Neural Information Processing Systems*, 4766–4775. 2017-Decem(Section 2).

Myers, T. A., & Norris, J. R. (2015). On the relationships between subtropical clouds and meteorology in observations and CMIP3 and CMIP5 models. *Journal of Climate*, *28*(8), 2945–2967. https://doi.org/10.1175/JCLI-D-14-00475.1

Myers, T. A., & Norris, J. R. (2016). Reducing the uncertainty in subtropical cloud feedback. *Geophysical Research Letters*, *43*(5), 2144–2148. https://doi.org/10.1002/2015GL067416

Myers, T. A., Scott, R. C., Zelinka, M. D., Klein, S. A., Norris, J. R., & Caldwell, P. M. (2021). Observational constraints on low cloud feedback reduce uncertainty of climate sensitivity. *Nature Climate Change*, *11*(6), 501–507. https://doi.org/10.1038/s41558-021-01039-0

Qu, X., Hall, A., Klein, S. A., & Deangelis, A. M. (2015). Positive tropical marine low-cloud cover feedback inferred from cloud-controlling factors. *Geophysical Research Letters*, *42*(18), 7767–7775. https://doi.org/10.1002/2015GL065627

Rayner, N. A., Parker, D. E., Horton, E. B., Folland, C. K., Alexander, L. V., Rowell, D. P., et al. (2003). Global analyses of sea surface temperature, sea ice, and night marine air temperature since the late nineteenth century. *Journal of Geophysical Research*, *108*(14). https://doi.org/10.1029/2002jd002670

Rieck, M., Nuijens, L., & Stevens, B. (2012). Marine boundary layer cloud feedbacks in a constant relative humidity atmosphere. *Journal of the Atmospheric Sciences*, *69*(8), 2538–2550. https://doi.org/10.1175/JAS-D-11-0203.1

Sandu, I., Stevens, B., & Pincus, R. (2010). On the transitions in marine boundary layer cloudiness. *Atmospheric Chemistry and Physics*, *10*(5), 2377–2391. https://doi.org/10.5194/acp-10-2377-2010

Seethala, C., Norris, J. R., & Myers, T. A. (2015). How has subtropical stratocumulus and associated meteorology changed since the 1980s? *Journal of Climate*, *28*(21), 8396–8410. https://doi.org/10.1175/jcli-d-15-0120.1

Soden, B. J., & Vecchi, G. A. (2011). The vertical distribution of cloud feedback in coupled ocean-atmosphere models. *Geophysical Research Letters*, *38*(12), L12704. https://doi.org/10.1029/2011GL047632

Tan, I., Storelvmo, T., & Zelinka, M. D. (2016). Observational constraints on mixed-phase clouds imply higher climate sensitivity. *Science*, *352*(6282), 224–227. https://doi.org/10.1126/science.aad5300

van der Dussen, J. J., de Roode, S. R., Dal Gesso, S., & Siebesma, A. P. (2015). An LES model study of the influence of the free tropospheric thermodynamic conditions on the stratocumulus response to a climate perturbation. *Journal of Advances in Modeling Earth Systems*, *7*(2), 670–691. https://doi.org/10.1002/2014MS000380

van der Dussen, J. J., de Roode, S. R., & Siebesma, A. P. (2016). How large-scale subsidence affects stratocumulus transitions. *Atmospheric Chemistry and Physics*, *16*(2), 691–701. https://doi.org/10.5194/acp-16-691-2016

Vial, J., Dufresne, J.-L., & Bony, S. (2013). On the interpretation of inter-model spread in CMIP5 climate sensitivity estimates. *Climate Dynamics*, *41*(11–12), 3339–3362. https://doi.org/10.1007/s00382-013-1725-9

Wall, C. J., Hartmann, D. L., & Ma, P. L. (2017). Instantaneous linkages between clouds and large-scale meteorology over the Southern Ocean in observations and a climate model. *Journal of Climate*, *30*(23), 9455–9474. https://doi.org/10.1175/JCLI-D-17-0156.1

Wood, R. (2012). Stratocumulus clouds. *Monthly Weather Review*, *140*(8), 2373–2423. https://doi.org/10.1175/MWR-D-11-00121.1

Wood, R., & Bretherton, C. S. (2006). On the relationship between stratiform low cloud cover and lower-tropospheric stability. *Journal of Climate*, *19*(24), 6425–6432. https://doi.org/10.1175/JCLI3988.1

Wyant, M. C., Bretherton, C. S., Rand, H. A., & Stevens, D. E. (1997). Numerical simulations and a conceptual model of the stratocumulus to trade cumulus transition. *Journal of the Atmospheric Sciences*, *54*(1), 168–192. https://doi.org/10.1175/1520-0469(1997)054<0168:nsaacm>2.0.co;2

Zhang, G. J., & McFarlane, N. A. (1995). Sensitivity of climate simulations to the parameterization of cumulus convection in the Canadian climate centre general circulation model. *Atmosphere-Ocean*, *33*(3), 407–446. https://doi.org/10.1080/07055900.1995.9649539

Zhang, H., Wang, M., Guo, Z., Zhou, C., Zhou, T., Qian, Y., et al. (2018). Low-cloud feedback in CAM5–CLUBB: Physical mechanisms and parameter sensitivity analysis. *Journal of Advances in Modeling Earth Systems*, *10*(11), 1–21. https://doi.org/10.1029/2018MS001423

Zhang, H., Zheng, Y., Lee, S. S., & Li, Z. (2023). Surface-atmosphere decoupling prolongs cloud lifetime under warm advection due to reduced entrainment drying. *Geophysical Research Letters*, *50*(10), 1–10. https://doi.org/10.1029/2022GL101663

Zhang, M., Bretherton, C. S., Blossey, P. N., Austin, P. H., Bacmeister, J. T., Bony, S., et al. (2013). CGILS: Results from the first phase of an international project to understand the physical mechanisms of low cloud feedbacks in single column models. *Journal of Advances in Modeling Earth Systems*, *5*(4), 826–842. https://doi.org/10.1002/2013MS000246

Zheng, Y., & Li, Z. (2019). Episodes of warm-air advection causing cloud-surface decoupling during the MARCUS. *Journal of Geophysical Research: Atmospheres*, *124*(22), 12227–12243. https://doi.org/10.1029/2019jd030835

Zheng, Y., Rosenfeld, D., & Li, Z. (2020). A more general paradigm for understanding the decoupling of stratocumulus-topped boundary layers: The importance of horizontal temperature advection. *Geophysical Research Letters*, *47*(14), e2020GL087697. https://doi.org/10.1029/2020gl087697

Zheng, Y., Zhang, H., Rosenfeld, D., Lee, S.-S., Su, T., & Li, Z. (2021). Idealized Large-eddy simulations of stratocumulus advecting over cold water. Part I: Boundary layer decoupling. *Journal of the Atmospheric Sciences*, *78*(12), 4089–4102. https://doi.org/10.1175/JAS-D-21-0108.1